EXCITED STATES $J^\pi = 1^+$ IN SPHERICAL NUCLEI

By S. Ćwiok and M. Wygonowska

Institute of Experimental Physics, University of Warsaw*

(Received July 7, 1972)

Energies, wave functions and M1 electromagnetic transition widths have been calculated for ^{55}Ni, $^{114, 116, 118, 120, 122, 124}$Sn, ^{138}Ba, ^{140}Ce, ^{142}Nd and ^{208}Pb with the use of the Saxon-Woods potential and "realistic" residual forces. Several excited states $J^\pi = 1^+$ in the energy region 2.3—12.4 MeV have been obtained for each nucleus. Some of these states are a coherent mixture of configurations generated by spin-orbit interaction and have a large width for M1 electromagnetic transitions.

1. Introduction

Recently, there has been considerable interest in spin-spin correlations induced by residual interactions in atomic nuclei. These correlations affect the magnitude of odd-mass nuclei magnetic moments in such a way that they differ noticeably from the values indicated by Schmidt diagrams [1, 2]. Spin polarization reduces considerably the probability of allowed β-decay between low-lying excited states [3].

Taking into account spin-spin interaction, Emery and Shapiro give evidence for M1 resonance at the energy region 5–8 MeV in even-even deformed nuclei [4]. Gabrakov *et al.* indicate that in even-even deformed nuclei this interaction produces excited $J^\pi = 1^+$ states, the strength function of which has a main maximum at 8–10 MeV and a second maximum at 6–8 MeV [5, 6, 7]. Calculations for ^{208}Pb have been carried out by Broglia *et al.* [8]. They report two excited $J^\pi = 1^+$ states at 5.84 MeV and 7.47 MeV.

The purpose of the present paper is to investigate excited states $J^\pi = 1^+$ in the energy region 3–12 MeV in ^{56}Ni, $^{114, 116, 118, 120, 122, 124}$Sn, ^{138}Ba, ^{140}Ce, ^{142}Nd and ^{208}Pb. These are the nuclei with one or both, neutron and proton, closed shells. Our results show that in all the quoted nuclei there exist a few excited states $J^\pi = 1^+$, some of them concentrating the main part of M1 electromagnetic transition.

* Address: Instytut Fizyki Doświadczalnej, Uniwersytet Warszawski, Hoża 69, 00–681 Warszawa, Poland.

2. Theoretical description

2.1. The Hamiltonian

After performing the Bogolyubov transformation

$$a_\alpha(\tau) = u_\alpha(\tau)b_\alpha(\tau)+v_\alpha(\tau)b^+_{\tilde{\alpha}}(\tau)$$
$$a_{\tilde{\alpha}}(\tau) = u_\alpha(\tau)b_{\tilde{\alpha}}(\tau)-v_\alpha(\tau)b^+_\alpha(\tau) \tag{1}$$

the nuclear Hamiltonian has the form:

$$H = U+\sum_{\alpha\tau} e_\alpha(\tau)b^+_\alpha(\tau)b_\alpha(\tau)+$$
$$+\tfrac{1}{4}\sum_{\alpha\beta\gamma\sigma\tau\tau'}\langle\alpha\beta|v|\gamma\sigma\rangle_a N(a^+_\alpha(\tau)a^+_\beta(\tau')a_\sigma(\tau')a_\gamma(\tau)). \tag{2}$$

Here U is the ground state energy. The second term describes independent quasi-particle excitations and the last term represents the quasi-particle residual interaction. τ is the izospin variable ($\tau = p, n$). The other Greek letters, α, β, γ and σ, stand for the complete set of quantum numbers necessary for specifying the single-particle level. In the case of the spherical potential, $\{\alpha\} = \{nljm\}$, where $nljm$ are the well known quantum numbers. $a^+(a)$ and $b^+(b)$ are particle and quasi-particle creation (annihilation) operators. $e_\alpha(\tau)$ is the quasi-particle energy given by the formula:

$$e_\alpha(\tau) = ((\varepsilon_\alpha(\tau)-\lambda(\tau))^2+\Delta^2(\tau))^{\frac{1}{2}} \tag{3}$$

where $\varepsilon_\alpha(\tau)$ is the single-particle energy, $\lambda(\tau)$ is the Fermi energy and Δ is the energy gap. N appearing in (2) stands for the normal product of quasi-particle operators.

2.2. Quasi-boson approximation

One can introduce the following two-quasi-particle operators $B^+_\tau(j_1j_2; J^\pi M)$ and its adjoints $B_\tau(j_1j_2; J^\pi M)$

$$B^+_\tau(j_1j_2; J^\pi M) = \sum_{m_1m_2}\langle j_1m_1j_2m_2|JM\rangle b^+_{j_1m_1}(\tau)b^+_{j_2m_2}(\tau)$$
$$B_\tau(j_1j_2; J^\pi M) = \sum_{m_1m_2}\langle j_1m_1j_2m_2|JM\rangle b_{j_2m_2}(\tau)b_{j_1m_1}(\tau). \tag{4}$$

Operator $B^+_\tau(j_1j_2; J^\pi M)$ creates a two-quasi-particle state of the total angular momentum J and parity π. In constructing the pairs (j_1, j_2), first all the quasi-particle states (j) are numbered in some convenient way (*e.g.*, increasing order of energy ε_j), and then in the pair (j_1, j_2) it is understood that $\varepsilon_{j_1} < \varepsilon_{j_2}$. We first show commutation relations which are used in the following calculations,

$$[B^+_\tau(j_1j_2; J^\pi M), B^+_{\tau'}(j'_1j'_2; J'^{\pi'}M')] = 0$$
$$[B_\tau(j_1j_2; J^\pi M), B^+_{\tau'}(j'_1j'_2; J'^{\pi'}M')] = \delta_{\tau\tau'}\delta_{J^\pi J'^{\pi'}}\delta_{j_1j'_1}\delta_{j_2j'_2}\delta_{MM'}+\hat{R}$$
$$[B_\tau(j_1j_2; J^\pi M), B_{\tau'}(j'_1j'_2; J'^{\pi'}M')] = 0 \tag{5}$$

where $\hat{R} \sim b^+_\alpha b_\beta$.

Except for the term $\hat{R}$ the B's behave like boson operators. In the quasi-boson approximation one puts $\hat{R} = 0$. It should be noted that the simplicity has been obtained at the cost of some violation of the exclusion principle. One can use the quasi-boson approximation in the case of a small number of excited quasi-particles, so that the probability that two quasi-particles are in the same state is also small.

2.3. Random phase approximation and Tamm-Dancoff approximation

In RPA and TDA the excited states are considered as one-phonon states. The fundamental assumption of the RPA [9] is that the excited states differ from the ground state by the presence or absence of one pair of quasi-particles. That means retaining the amplitudes:

$$X^{(n)}_{j_1 j_2}(J^\pi, \tau) = \langle \psi_{EnJ^\pi M} | B^+_\tau(j_1 j_2; J^\pi M) | \psi_0 \rangle$$
$$Y^{(n)}_{j_1 j_2}(J^\pi, \tau) = \langle \psi_{EnJ^\pi M} | B_\tau(j_1 j_2; \widetilde{J^\pi M}) | \psi_0 \rangle. \tag{6}$$

Hence, the general form of the excited-state vector

$$|\psi_{EnJ^\pi M}\rangle = \sum_{(j_1, j_2)\tau} [X^{(n)}_{j_1 j_2}(J^\pi, \tau) B^+_\tau(j_1 j_2; J^\pi M) -$$
$$- Y^{(n)}_{j_1 j_2}(J^\pi, \tau) B_\tau(j_1 j_2; \widetilde{J^\pi M})] |\psi_0\rangle \equiv Q^+_{EnJ^\pi M} |\psi_0\rangle \tag{7}$$

where

$$Q^+_{EnJ^\pi M} = \sum_{(j_1, j_2)\tau} [X^{(n)}_{j_1 j_2}(J^\pi, \tau) B^+_\tau(j_1 j_2; J^\pi M) -$$
$$- Y^{(n)}_{j_1 j_2}(J^\pi, \tau) B_\tau(j_1 j_2; \widetilde{J^\pi M})] \tag{8}$$

is an operator creating a one-phonon state.

From the orthonormality condition for the excited states one obtains using the commutation relations (5) with the following expression:

$$\sum_{(j_1, j_2)} [X^{(n)}_{j_1 j_2}(J^\pi, \tau) X^{(n')}_{j_1 j_2}(J^\pi, \tau) - Y^{(n)}_{j_1 j_2}(J^\pi, \tau) Y^{(n')}_{j_1 j_2}(J^\pi, \tau)] = \delta_{nn'}. \tag{9}$$

The RPA ground state $|\psi_0\rangle$ is defined by

$$B_\tau(j_1 j_2; J^\pi M) |\psi_0\rangle = 0.$$

2.4. The fundamental equations of RPA

The equations which are obeyed by X and Y can be derived most easily by computing the comutators $[H, B^+]$ and $[H, B]$ and taking their matrix elements with respect to $|\psi_{EnJ^\pi M}\rangle$ and $|\psi_0\rangle$.

By the use of Wick's theorem one obtains the following expressions:

$$[H, B^+_\tau(j_1 j_2; J^\pi M)] = (e_{j_1}(\tau) + e_{j_2}(\tau)) B^+_\tau(j_1 j_2; J^\pi M) +$$
$$+ \sum_{(j_3, j_4)\tau'} [2 \times P_{\tau\tau'}(j_1 j_2; j_3 j_4; J^\pi M) +$$

$$+2\times R_{\tau\tau'}(j_1 j_2; j_3 j_4; J^\pi)B_{\tau'}(j_3 j_4; \widetilde{J^\pi M})]+\hat{T}(J^\pi M) \tag{10a}$$

$$[H, B_\tau(j_1 j_2; \widetilde{J^\pi M})] = -(e_{j_1}(\tau)+e_{j_2}(\tau))B_\tau(j_1 j_2; \widetilde{J^\pi M})-$$

$$-\sum_{(j_3,j_4)\tau'}[2\times P_{\tau\tau'}(j_1 j_2; j_3 j_4; J^\pi)B_{\tau'}(j_3 j_4; \widetilde{J^\pi M})+$$

$$+2\times R_{\tau\tau'}(j_1 j_2; j_3 j_4; J^\pi)B^+_{\tau'}(j_3 j_4; J^\pi M)]-\hat{T}(\widetilde{J^\pi M}) \tag{10b}$$

where $\hat{T}$ denotes the sum of operators of the B^+b^+b, b^+bB and b^+b type.

Following the prescribed way one obtains the required RPA equations:

$$(e_{j_1}(\tau)+e_{j_2}(\tau))X^{(n)}_{j_1 j_2}(J^\pi,\tau)+\sum_{(j_3,j_4)\tau'}[2\times P_{\tau\tau'}(j_1 j_2; j_3 j_4; J^\pi)\times$$

$$\times X^{(n)}_{j_3 j_4}(J^\pi,\tau')+2\times R_{\tau\tau'}(j_1 j_2; j_3 j_4; J^\pi)Y^{(n)}_{j_3 j_4}(J^\pi,\tau')] =$$

$$=E_n(J^\pi)X^{(n)}_{j_1 j_2}(J^\pi,\tau)$$

$$(e_{j_1}(\tau)+e_{j_2}(\tau))Y^{(n)}_{j_1 j_2}(J^\pi,\tau)+\sum_{(j_3,j_4)\tau}[2\times P_{\tau\tau'}(j_1 j_2; j_3 j_4; J^\pi)\times$$

$$\times Y^{(n)}_{j_3 j_4}(J^\pi,\tau')+2\times R_{\tau\tau'}(j_1 j_2; j_3 j_4; J^\pi)X^{(n)}_{j_3 j_4}(J^\pi,\tau')] =$$

$$=-E_n(J^\pi)Y^{(n)}_{j_1 j_2}(J^\pi,\tau). \tag{11}$$

Matrix elements of $\hat{T}$ can be neglected according to fundamental assumptions of the RPA. The coefficients P and R are defined by the irreducible matrix elements of the residual interaction

$$2\times P_{\tau\tau}(j_1 j_2; j_3 j_4; J^\pi) = [u_{j_1}(\tau)u_{j_2}(\tau)u_{j_3}(\tau)u_{j_4}(\tau)+$$

$$+v_{j_1}(\tau)v_{j_2}(\tau)v_{j_3}(\tau)v_{j_4}(\tau)](2\times J+1)^{-1/2}\langle j_1(\tau)j_2(\tau); J^\pi||v_{\tau\tau}||j_3(\tau)j_4(\tau); J^\pi\rangle_a+$$

$$+[u_{j_1}(\tau)v_{j_2}(\tau)u_{j_3}(\tau)v_{j_4}(\tau)+v_{j_1}(\tau)u_{j_2}(\tau)v_{j_3}(\tau)u_{j_4}(\tau)]\times$$

$$\times\sum_{J'}(-1)^{J'+j_2+j_3}(2J'+1)^{1/2}\begin{Bmatrix} j_1 j_2 J \\ j_3 j_4 J'\end{Bmatrix}\langle j_1(\tau)j_4(\tau); J'||v_{\tau\tau}||j_2(\tau)j_3(\tau); J'\rangle_a+$$

$$+[v_{j_1}(\tau)u_{j_2}(\tau)u_{j_3}(\tau)v_{j_4}(\tau)+u_{j_1}(\tau)v_{j_2}(\tau)v_{j_3}(\tau)u_{j_4}(\tau)]\times\sum_{J'}(-1)^{J'+J+j_2+j_3}\times$$

$$\times(2J'+1)^{1/2}\begin{Bmatrix} j_1 j_2 J \\ j_4 j_3 J'\end{Bmatrix}\langle j_1(\tau)j_3(\tau); J'||v_{\tau\tau}||j_2(\tau)j_4(\tau); J'\rangle_a \tag{12a}$$

$$2\times R_{\tau\tau}(j_1 j_2; j_3 j_4; J^\pi) = -[u_{j_1}(\tau)u_{j_2}(\tau)v_{j_3}(\tau)v_{j_4}(\tau)+$$

$$+v_{j_1}(\tau)v_{j_2}(\tau)u_{j_3}(\tau)u_{j_4}(\tau)](2J+1)^{-1/2}\langle j_1(\tau)j_2(\tau); J^\pi||v_{\tau\tau}||j_3(\tau)j_4(\tau); J^\pi\rangle_a+$$

$$+[u_{j_1}(\tau)v_{j_2}(\tau)u_{j_3}(\tau)v_{j_4}(\tau)+v_{j_1}(\tau)u_{j_2}(\tau)v_{j_3}(\tau)u_{j_4}(\tau)]\times\sum_{J'}(-1)^{J+J'+j_2+j_3}\times$$

$$\times(2J'+1)^{1/2}\begin{Bmatrix} j_1 j_2 J \\ j_4 j_3 J'\end{Bmatrix}\langle j_1(\tau)j_3(\tau); J'||v_{\tau\tau}||j_2(\tau)j_4(\tau); J'\rangle_a+$$

$$+[u_{j_1}(\tau)v_{j_2}(\tau)v_{j_3}(\tau)u_{j_4}(\tau)+v_{j_1}(\tau)u_{j_2}(\tau)u_{j_3}(\tau)v_{j_4}(\tau)]\times\sum_{J'}(-1)^{J'+j_2+j_3}\times$$

$$\times(2J'+1)^{1/2}\begin{Bmatrix}j_1 j_2 J\\ j_3 j_4 J'\end{Bmatrix}\langle j_1(\tau)j_4(\tau);J'||v_{\tau\tau}||j_2(\tau)j_3(\tau);J'\rangle_a \tag{12b}$$

for proton-proton or neutron-neutron interaction, and

$$2\times P_{pn}(\varphi j_1 j_2;j_3 j_4;J^\pi)=[u_{j_1}(p)v_{j_2}(p)u_{j_3}(n)v_{j_4}(n)+v_{j_1}(p)u_{j_2}(p)v_{j_3}(n)u_{j_4}(n)]\times$$

$$\times\sum_{J'}(-1)^{J'+j_2+j_3}(2J'+1)\begin{Bmatrix}j_1 j_2 J\\ j_3 j_4 J'\end{Bmatrix}\langle j_2(p)j_3(n);J'||v_{pn}||j_1(p)j_4(n);J'\rangle+$$

$$+[u_{j_1}(p)v_{j_2}(p)v_{j_3}(n)u_{j_4}(n)+v_{j_1}(p)u_{j_2}(p)u_{j_3}(n)v_{j_4}(n)]\times$$

$$\times\sum_{J'}(-1)^{J+J'+j_2+j_3}(2J'+1)\begin{Bmatrix}j_1 j_2 J\\ j_4 j_3 J'\end{Bmatrix}\times$$

$$\times\langle j_2(p)j_4(n);J'||v_{pn}||j_1(p)j_3(n);J'\rangle \tag{12c}$$

$$2\times R_{pn}(j_1 j_2;j_3 j_4;J^\pi)=[v_{j_1}(p)u_{j_2}(p)u_{j_3}(n)v_{j_4}(n)+u_{j_1}(p)v_{j_2}(p)v_{j_3}(n)u_{j_4}(n)]\times$$

$$\times\sum_{J'}(-1)^{J'+j_2+j_3}(2J+1)^{1/2}\begin{Bmatrix}j_1 j_2 J\\ j_3 j_4 J'\end{Bmatrix}\langle j_2(p)j_3(n);J'||v_{pn}||j_1(p)j_4(n);J'\rangle+$$

$$+[v_{j_1}(p)u_{j_2}(p)v_{j_3}(n)u_{j_4}(n)+u_{j_1}(p)v_{j_2}(p)u_{j_3}(n)v_{j_4}(n)]\times$$

$$\times\sum_{J'}(-1)^{J'+j_2+j_3+J}(2J'+1)^{1/2}\begin{Bmatrix}j_1 j_2 J\\ j_4 j_3 J'\end{Bmatrix}\times$$

$$\times\langle j_2(p)j_4(n);J'||v_{pn}||j_1(p)j_3(n);J'\rangle \tag{12d}$$

for proton-neutron interaction.

One has the symmetry relations:

$$P_{\tau\tau'}(\alpha;\beta;J^\pi)=P_{\tau'\tau}(\beta;\alpha;J^\pi)$$
$$R_{\tau\tau'}(\alpha;\beta;J^\pi)=R_{\tau'\tau}(\beta;\alpha;J^\pi) \tag{13}$$

resulting from the definitions of P and R.

The RPA equations can be summarized as

$$\begin{bmatrix}A-E\times I, & B\\ -B & , -A-E\times 1\end{bmatrix}\begin{bmatrix}X\\ Y\end{bmatrix}=0 \tag{14}$$

in obvious notation

$$A=2\times P+e\times I$$
$$B=2\times R. \tag{15}$$

The matrices A and B are symmetrical and real. Their order is equal to the number of two-quasi-particle excitations. The eigen-value problem in RPA is equivalent to diagonalization of a $2n$ by $2n$ matrix, n denoting the number of two-quasi-particle excitations.

It can be shown [11] that this problem may be reduced to the diagonalization of the n by n, symmetrical and real matrix N or M defined as

$$N = A+B \quad \text{and} \quad M = A-B.$$

Following the work [11] one obtains the expression for X and Y,

$$X^{(n)} = \tfrac{1}{2}T \times \left(\frac{1}{E_n} \times N_d^{1/2} + N_d^{-1/2}\right) \times V''^{(n)}$$

$$Y^{(n)} = \tfrac{1}{2}T \times \left(\frac{1}{E_n} \times N_d^{1/2} - N_d^{-1/2}\right) \times V''^{(n)} \tag{16}$$

where matrix T diagonalizes N:

$$\tilde{T}NT = Nd.$$

$V''^{(n)}$ nad E_n^2 are the eigenvectors and eigenvalues of the real symmetrical matrix $\{N_d^{1/2}\tilde{T}MTN_d^{1/2}\}$. From the normalization condition (9) one obtains the equation:

$$(\tilde{V}''^{(n)}, V''^{(n)}) = E_n. \tag{17}$$

TDA equations can be obtained from (11) putting $Y = 0$.

3. The width of the magnetic dipole transition

In the quasi-particle representation we get the following expression for the magnetic dipole operator:

$$\hat{\mathcal{M}}^{M1}_{J^\pi=1^+,M} = \left(\frac{3}{4\pi}\right)^{1/2} \frac{e\hbar}{2m_pc} \sum_{(j_1,j_2)\tau} \frac{1}{\sqrt{3}} [v_{j_1}(\tau)u_{j_2}(\tau) - u_{j_1}(\tau)v_{j_2}(\tau)] \times$$

$$\times \langle j_1(\tau)||\bar{\mu}(\tau)||j_2(\tau)\rangle [B_\tau^+(j_1j_2; J^\pi = 1^+, M) -$$

$$- B_\tau(j_1j_2; \overline{J^\pi = 1^+, M})] + \hat{\mathcal{M}}^{M1}_{J^\pi=1^+,M}(r) \tag{18}$$

where $\bar{\mu}$ is the magnetic dipole moment,

$$\bar{\mu}(\tau) = g_l(\tau)\bar{l} + g_s(\tau)\bar{s}$$

and

$$g_l = 1, \quad g_s = \quad 5.5855 \quad \text{for a proton,}$$

$$g_l = 0, \quad g_s = -3.8263 \quad \text{for a neutron.}$$

The last term of the equation (18) is a component which does not lead to transitions between excited and ground states. The reduced transition probability has the form:

$$B^{M1}_{0^+\to 1^+} = \frac{1}{2\times 0+1}\,|\langle\psi_{EnJ^\pi=1^+}||\,\hat{\mathcal{M}}^{M1}_{\pi=1^+}||\psi_0\rangle|^2 =$$

$$= \left(\frac{e\hbar}{2m_pc}\right)^2 \frac{3}{4\pi}\left|\sum_{(j_1,j_2)\tau}\frac{1}{\sqrt{3}}\left[v_{j_1}(\tau)u_{j_2}(\tau)-u_{j_1}(\tau)v_{j_2}(\tau)\right]\times\right.$$

$$\left.\times\langle j_1(\tau)||\bar{\mu}(\tau)||j_2(\tau)\rangle\left[X^{(n)}_{j_1j_2}(J^\pi=1^+,\tau)-Y^{(n)}_{j_1j_2}(J^\pi=1^+,\tau)\right]\right|^2. \tag{19}$$

Therefore, the width of the magnetic dipole transition can be written as

$$\Gamma^{M1}_{0^+\to 1^+} = \tfrac{1}{3}\hbar\omega\times\alpha\times\left(\frac{\hbar\omega}{m_pc^2}\right)^2\left|\sum_{(j_1,j_2)\tau}\frac{1}{\sqrt{3}}\left[v_{j_1}(\tau)u_{j_2}(\tau)-u_{j_1}(\tau)v_{j_2}(\tau)\right]\times\right.$$

$$\left.\times\langle j_1(\tau)||\bar{\mu}(\tau)||j_2(\tau)\rangle\left[X^{(n)}_{j_1j_2}(J^\pi=1^+,\tau)-Y^{(n)}_{j_1j_2}(J^\pi=1^+,\tau)\right]\right|^2 \tag{20}$$

where α is the fine-structure constant. Γ is obtained in MeV if one puts transition energy $\hbar\omega$ and proton mass m_pc^2 in MeV.

The right-hand side of the expression (19) is the squared sum of thr terms which correspond to various two-quasi-particle states. It is possible that for some excited states this sum is coherent or nearly coherent. Such a state has a large M1 transition width as compared with the others, and is usually called a "collective state".

4. Numerical calculations

The numerical calculation has been performed for ^{56}Ni, $^{114,\,116,\,118,\,120,\,122,\,124}$Sn, ^{138}Ba, ^{140}Ce, ^{142}Nd and ^{208}Pb. The excitation energies E, amplitudes X, Y and M1 transition widths Γ were computed by the use of a realistic residual potential. The Saxon-Woods potential [12]

$$V_{N,Z}(r) = -V_0^{N,Z}f(r)$$

where

$$f(r) = \left[1+\exp\left(\frac{r-R}{\alpha}\right)\right]^{-1}$$

and spin-orbital potential

$$V_{\text{s.o.}}(r) = -\kappa V_0^{N,Z}\frac{1}{r}\frac{df}{dr}$$

has been assumed for single-particle state calculations. The parameters are as follows [18]:

$$R = r_0A^{1/3},\ r_0 = 1.24\text{ fm},\ \alpha = 0.63\text{ fm},$$

$$V_0^{N,Z} = V_0\times\left(1\mp 0.63\times\frac{N-Z}{A}\right),\quad V_0 = 53\text{ MeV},$$

$$\kappa = 0.263\times\left(1+2\times\frac{N-Z}{A}\right).$$

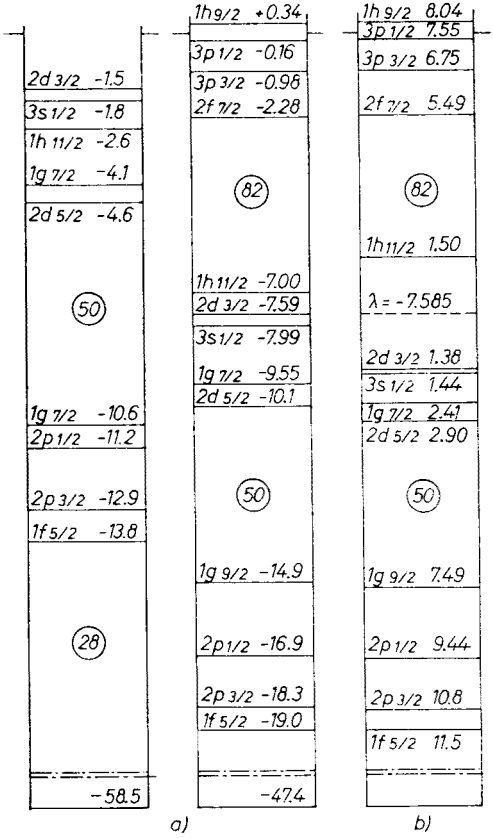

Fig. 1

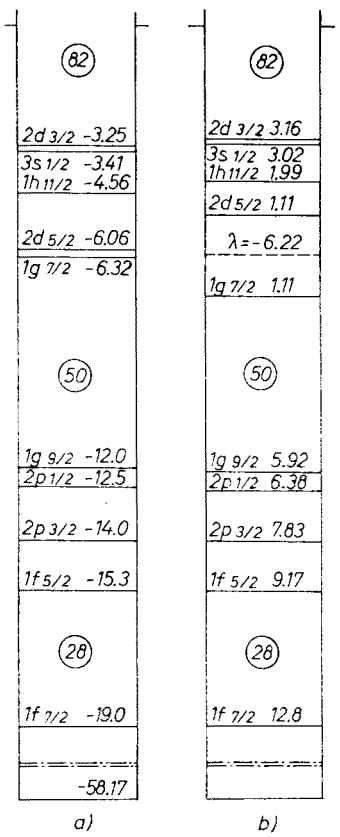

Fig. 2

Fig. 1. Single-particle level scheme for ^{120}Sn. a) proton and neutron particle levels, b) quasi-particle neutron levels

Fig. 2. Single-particle proton level scheme for ^{140}Ce. a) particle levels, b) quasi-particle levels

The superconducting state appears in the neutron shell for Sn and in the proton shell for Ba, Ce and Nd. The strength of the pairing forces G has been fitted to he condensation energy numerically [14]. The levels $1f_{5/2}$, $2p_{3/2}$, $2p_{1/2}$, $1g_{9/2}$, $2d_{5/2}$, $1g_{7/2}$ $3s_{1/2}$, $2d_{3/2}$, $1h_{11/2}$, $2f_{7/2}$, $3p_{3/2}$, $1h_{9/2}$ were taken into account for the Sn isotopes and $1f_{7/2}$, $1f_{5/2}$, $2p_{3/2}$, $2p_{1/2}$, $1g_{9/2}$, $1g_{7/2}$, $2d_{5/2}$, $1h_{11/2}$, $3s_{1/2}$, $2d_{3/2}$ for Ba, Ce and Nd. In Fig. 3 the parameter G is plotted versus mass-number A for Sn isotopes. In the case of ^{120}Sn the G value does not fit the curve, but has a considerably lower value. This is due to the shell effect (closed $2d_{3/2}$ level), so that the value $G = 0.1752$ resulting from interpolation has been used. The parameters G, λ and Δ for the nuclei under consideration are listed in Table I.

For excited state $J^\pi = 1^+$ calculations all the two-quasi-particle states in two neighbouring shells have been taken into account. These are as follows:

a) ^{56}Ni: $1f_{7/2}$–$1f_{5/2}$ for neutrons and protons,

b) Sn: $1g_{9/2}$–$1g_{7/2}$, $2d_{5/2}$–$1g_{7/2}$, $2d_{5/2}$–$2d_{3/2}$, $3s_{1/2}$–$2d_{3/2}$, $1h_{11/2}$–$1h_{9/2}$ for neutrons and $1g_{9/2}$–$1g_{7/2}$ for protons,

c) ^{138}Ba, ^{140}Ce, ^{142}Nd: $1g_{9/2}$–$1g_{7/2}$, $1g_{7/2}$–$2d_{5/2}$, $2d_{5/2}$–$2d_{3/2}$, $3s_{1/2}$–$2d_{3/2}$ for protons and $1h_{11/2}$–$1h_{9/2}$ for neutrons,

d) ^{208}Pb: $1i_{13/2}$–$1i_{11/2}$ for neutrons and $1h_{11/2}$–$1h_{9/2}$ for protons.

The configurations and corresponding energies for ^{120}Sn and ^{140}Ce are summarized in Tables II and III (Fig. 1, 2).

TABLE I

The parameters G, Δ and λ

Nucleus	G (MeV)	Δ (MeV)	λ (MeV)	Nucleus	G (MeV)	Δ (MeV)	λ (MeV)
^{114}Sn	0.180	1.375	−8.783	^{122}Sn	0.1725	1.446	−7.298
^{116}Sn	0.179	1.266	−8.362	^{124}Sn	0.1685	1.358	−6.992
^{118}Sn	0.1775	1.471	−7.933	^{138}Ba	0.1590	0.957	−7.055
^{120}Sn	0.169	—	—	^{140}Ce	0.1690	1.107	−6.219
	0.1752	1.478	−7.587	^{142}Nd	0.1752	1.188	−5.333

TABLE II

Two-quasi-particle configurations in ^{120}Sn

Quasi-particle state [1]	e_1 (MeV)	v_1	u_1	Quasi-particle state [2]	e_2 (MeV)	v_2	u_2	$2qp$ excitation energy (MeV)
$1g_{9/2}$	7,51	0.995	0.099	$1g_{7/2}$	2.46	0.949	0 317	9.97
$2d_{5/2}$	2 95	0.966	0.260	$1g_{7/2}$	2.46	0.949	0.317	5.41
$2d_{5/2}$	2.95	0.966	0.260	$2d_{3/2}$	1.48	0.709	0.705	4.43
$3s_{1/2}$	1.53	0.795	0.606	$2d_{3/2}$	1.48	0.709	0.705	3.01
$1h_{11/2}$	1.59	0.562	0.827	$1h_{9/2}$	8.06	0.092	0.996	9.65
$1g_{9/2}$[a]	−10.61	1.000	0.000	$1g_{7/2}$[a]	−4.11	0.000	1.000	6.50

[a] proton states.

TABLE III

Two-quasi-particle configurations in ^{140}Ce

Quasi-particle state [1]	e_1 (MeV)	v_1	u_1	Quasi-particle state [2]	e_2 (MeV)	v_2	u_2	$2qp$ excitation energy (MeV)
$1g_{9/2}$	5.92	0.996	0.094	$1g_{7/2}$	1.11	0.738	0.675	7.03
$1g_{7/2}$	1.11	0.738	0.675	$2d_{5/2}$	1.12	0.656	0.755	2.23
$2d_{5/2}$	1.12	0.656	0.755	$2d_{3/2}$	3.17	0.178	0.984	4.29
$3s_{1/2}$	3.02	0.187	0.982	$2d_{3/2}$	3.17	0.178	0.984	6.19
$1h_{11/2}$[b]	−10.44	1.000	0.000	$1h_{9/2}$	−3.68	0.000	1.000	6.76

[b] neutron states.

The residual potential used for calculating P and R has the form [15]:

$$v(r_{12}) = V_0 \exp(-r_{12}/\mu^2)\,[a_0 + a_\sigma \times (\bar{\sigma}(1)\cdot\bar{\sigma}(2)) + a_\tau \times (\bar{\tau}(1)\cdot\bar{\tau}(2)) + a_{\sigma\tau} \times (\bar{\sigma}(1)\cdot\bar{\sigma}(2)) \times (\bar{\tau}(1)\cdot\bar{\tau}(2))] \tag{21}$$

with parameters $V_0 = -40$ MeV, $\mu = 1.67$ fm, $a_0 = 0$ and $a_\tau = 0$.

The parameters a_σ and a_τ are those that gave the best fit to the magnetic moments of ^{59}Co and ^{207}Pb (ground state) [16] and the energy of excited states $J^\pi = 1^+$ in lead [17].

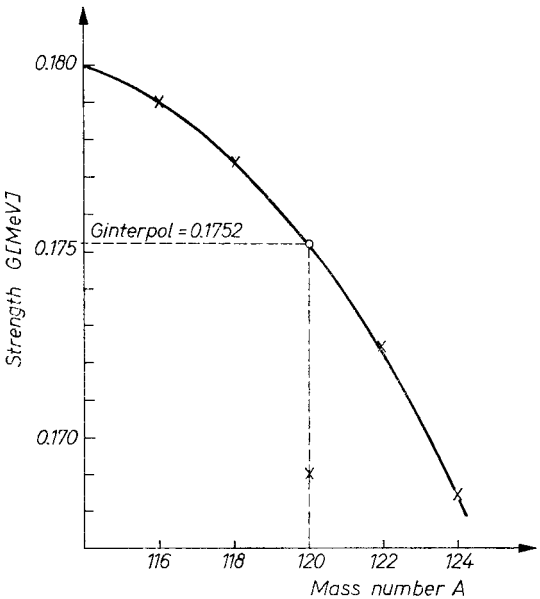

A	G[MeV]
114	0.180*
116	0.179
118	0.1775
120	0.169
	0.1752*
122	0.1725
124	0.1685

Fig. 2. Strength of pairing forces G *versus* mass number A for tin isotopes. * — Values resulting from interpolation

Polarization effects leading to a renormalization of magnetic moment were developed in the perturbation theory. In the first case it was assumed that single-particle movement induces core polarization by virtual excitations of $1p$–$1h$ pairs on the orbits resulting from spin-orbit splitting when $J^\pi = 1^+$ in the pair. In the second case it was adopted that residual interaction leads to collective states $J^\pi = 1^+$. Coupling of these collective states to orbital single-particle motion results in renormalization of single-particle magnetic

moment. Both approaches give approximately the same results. The magnetic moment fit leaves us with several sets of parameters, as core polarization effects are linear with a_σ and $a_{\sigma\tau}$. Fitting to the energy of excited states $J^\pi = 1^+$ in lead allows us to fix the values of -0.1 and -0.2 to the parameters a_σ and $a_{\sigma\tau}$.

TABLE IV

Structure and $\Gamma^{M1}_{0^+\to 1^+}$ widths of excited states $J^\pi = 1^+$ in ^{56}Ni and ^{208}Pb

Nucleus		Energy (MeV)	$\Gamma^{M1}_{0^+\to 1^+}$ (eV)	$\Gamma^{M1*}_{0^+\to 1^+}$ (W. u.)	*nn* $1f_{7/2}-1f_{5/2}$		*pp* $1f_{7/2}-1f_{5/2}$	
					$X\times 10^3$	$Y\times 10^3$	$X\times 10^3$	$Y\times 10^3$
^{56}Ni	RPA	7.19 8.90	0.2 68.3	0.03 4.68	824 −582	132 −32	592 816	110 66
	TDA	7.62 8.99	0.6 80.9	0.06 5.37	832 −555		555 832	
					nn $1i_{13/2}-1i_{11/2}$		*pp* $1h_{11/2}-1h_{9/2}$	
^{208}Pb	RPA	6.74 7.82	1.5 79.8	0.24 8.05	617 793	85 51	797 −622	960 −28
	TDA	6.96 7.87	2.6 90.3	0.37 8.92	591 807		807 −591	

The single-particle energy of ^{208}Pb is taken from the experimental work [13].

* $\Gamma^{M1}_{0^+\to 1^+}$ in W. u. is defined as $\Gamma^{M1}_{0^+\to 1^+}/\Gamma^{M1}_W$, where $\Gamma^{M1}_W = 2.072\times 10^{-8} E_\gamma^3$, Γ^{M1}_W is in eV and E_γ in MeV.

Let us make a Legendre expansion of $V_0 \exp(-r_{12}^2/\mu^2)$,

$$V_0 \exp(-r_{12}^2/\mu^2) = \sum_{L=0}^{\infty} \frac{4\pi}{2\times L+1} v_L(r_1, r_2)\,(Y_L(\hat{r}_1)\cdot Y_L(\hat{r}_2)). \tag{22}$$

In the numerical computation higher order terms are neglected. Terms with $L = 0$, 2 and 4 are retained in the case of Ni and Pb, whereas for the other nuclei terms with $L = 0$, and 2. For all the nuclei in question but Sn isotopes, the contribution of odd L is excluded by selection rules. In the case of Sn the odd-multipole admixture is due to exchange terms of the coupling of $1h_{11/2}$–$1h_{9/2}$ to the other configurations. This admixture is very small [19].

In our calculation radial integrals F^L derived for ^{116}Sn have been used in the ^{114}Sn case and F^L derived for ^{120}Sn in the ^{118}Sn and ^{122}Sn cases. We can do this because the radial wave function varies very slowly with mass number A, as one can deduce by comparing Tables VI and XI.

TABLE V

Structure and $\Gamma^{M1}_{0^+\to 1^+}$ widths of excited states $J^\pi = 1^+$ in ^{114,116,118}Sn obtained in RPA

Nucleus	Energy (MeV)	$\Gamma^{M1}_{0^+\to 1^+}$ (eV)	$\Gamma^{M1}_{0^+\to 0^+}$ (W. u.)	nn $1g_{9/2}-1g_{7/2}$		nn $2d_{5/2}-2d_{3/2}$		nn $1h_{11/2}-1h_{9/2}$		pp $1g_{9/2}-1g_{7/2}$	
				$X\times 10^3$	$Y\times 10^3$	$X\times 10^3$	$Y\times 10^3$	$X\times 10^3$	$Y\times 10^3$	$X\times 10^3$	$Y\times 10^3$
^{114}Sn	4.39	0.7	0.42	−54	18	997	42	−11	8	81	32
	8.22	19.8	1.72	−513	−22	38	−30	−32	−12	−863	−92
	9.02	36.1	2.37	856	2	86	5	−69	1	−506	−31
	12.43	14.5	0.37	43	6	19	8	997	3	−60	6
^{116}Sn	4.32	0.7	0.42	41	−14	−997	−43	16	−11	−82	−33
	8.19	32.2	2.83	−273	−17	62	−26	−67	−14	−963	−98
	9.27	15.8	0.96	−959	−3	−60	−7	89	−3	263	10
	11.49	18.2	0.58	67	6	27	10	994	5	−86	6
^{118}Sn	4.73	0.6	0.28	32	−10	−997	−28	24	−8	−82	−30
	8.28	35.8	3.05	−114	−12	70	−23	−112	−15	−986	−97
	9.98	4.7	0.23	−960	−7	−34	−5	255	15	109	1
	10.97	35.7	1.30	238	−11	43	6	960	7	−140	6

TABLE VI

Structure and $\Gamma^{M1}_{0^+\to 1^+}$ widths of excited states $J^\pi = 1^+$ in ^{120,122,124}Sn obtained in RPA

Nucleus	Energy (MeV)	$\Gamma^{M1}_{0^+\to 1^+}$ (eV)	$\Gamma^{M1}_{0^+\to 1^+}$ (W. u.)	nn $1g_{9/2}-1g_{7/2}$		nn $2d_{5/2}-2d_{3/2}$		nn $1h_{11/2}-1h_{9/2}$		pp $1g_{9/2}-1g_{7/2}$	
				$X\times 10^3$	$Y\times 10^3$	$X\times 10^3$	$Y\times 10^3$	$X\times 10^3$	$Y\times 10^3$	$X\times 10^3$	$Y\times 10^3$
^{120}Sn	4.91	0.5	0.21	−26	6	997	21	−25	13	79	27
	8.31	33.8	2.84	−109	−17	67	−22	−174	−22	−982	−97
	10.26	6.3	0.28	−677	−19	6	4	735	7	−55	0
	10.66	40.7	1.62	−729	−29	−51	−10	−656	−14	192	−5
^{122}Sn	5.09	0.4	0.15	−23	6	997	16	−36	9	74	25
	8.34	29.8	2.48	65	8	−59	19	242	27	972	97
	10.03	37.4	1.79	285	11	−43	−3	−935	−23	210	2
	11.00	21.6	0.78	−956	1	−41	−5	−261	4	126	−5
^{124}Sn	5.21	0.3	0.10	20	−4	−997	−12	32	−13	−67	−22
	8.35	23.0	1.91	−49	−11	49	−20	−334	−34	−946	−97
	9.74	58.4	3.05	137	−4	−49	−7	−936	−23	321	8
	11.28	11.0	0.37	989	2	29	4	113	10	−89	4

TABLE VII

Structure and $\Gamma^{M1}_{0^+\to 1^+}$ widths of excited states $J^\pi = 1^+$ in ^{138}Ba, ^{140}Ce and ^{142}Nd obtained in RPA

Nucleus	Energy (MeV)	$\Gamma^{M1}_{0^+\to 1^+}$ (eV)	$\Gamma^{M1}_{0^+\to 1^+}$ (W. u.)	*pp* $1g_{9/2}-1g_{7/2}$		*pp* $2d_{5/2}-2d_{3/2}$		*nn* $1h_{11/2}-1h_{9/2}$	
				$X\times 10^3$	$Y\times 10^3$	$X\times 10^3$	$Y\times 10^3$	$X\times 10^3$	$Y\times 10^3$
^{138}Ba	4.88	0.5	0.22	91	−21	−995	−17	−46	−17
	7.75	2.4	0.25	−888	−59	−63	−30	−466	−68
	8.97	77.8	5.21	−456	1	−82	1	889	65
^{140}Ce	4.82	0.7	0.31	81	−21	−996	−21	−56	−20
	7.75	0.6	0.06	−876	−43	−47	−29	−488	−68
	8.80	67.3	4.77	−478	4	−87	2	876	67
^{142}Nd	4.67	0.9	0.42	66	−20	−997	−27	−65	−24
	7.83	0.5	0.05	−811	−30	−18	−28	−590	−74
	8.64	56.7	4.24	−582	4	−89	1	811	61

TABLE VIII

Structure and $\Gamma^{M1}_{0^+\to 1^+}$ widths of excited states $J^\pi = 1^+$ in ^{114,116,118}Sn obtained in TDA

Nucleus	Energy (MeV)	$\Gamma^{M1}_{0^+\to 1^+}$ (eV)	$\Gamma^{M1}_{0^+\to 1^+}$ (W. u.)	*nn* $1g_{9/2}-1g_{7/2}$	*nn* $2d_{5/2}-2d_{3/2}$	*nn* $1h_{11/2}-1h_{9/2}$	*pp* $1g_{9/2}-1g_{7/2}$
				$X\times 10^3$	$X\times 10^3$	$X\times 10^3$	$X\times 10^3$
^{114}Sn	4.42	0.8	0.43	−61	996	−14	64
	8.38	21.4	1.75	568	−18	22	822
	9.04	44.3	2.89	−820	−85	70	562
	12.43	14.2	0.36	−44	−20	−997	57
^{116}Sn	4.36	0.8	0.44	46	−996	19	−65
	8.36	39.9	3.29	−285	48	−59	−956
	9.28	17.7	1.07	−955	−61	90	276
	11.49	17.9	0.57	−69	−28	−994	81
^{118}Sn	4.75	0.6	0.28	34	−997	26	−66
	8.44	45.0	3.61	143	−57	106	982
	9.98	4.7	0.23	961	34	−252	−111
	10.98	34.7	1.27	235	43	962	−135

TABLE IX

Structure and $\Gamma^{M1}_{0^+\to 1^+}$ widths of excited states $J^\pi = 1^+$ in ^{120,122,124}Sn obtained in TDA

Nucleus	Energy (MeV)	$\Gamma^{M1}_{0^+\to 1^+}$ (eV)	$\Gamma^{M1}_{0^+\to 1^+}$ (W. u.)	nn $1g_{9/2}-1g_{7/2}$	nn $2d_{5/2}-2d_{3/2}$	nn $1h_{11/2}-1h_{9/2}$	pp $1g_{9/2}-1g_{7/2}$
				$X\times 10^3$	$X\times 10^3$	$X\times 10^3$	$X\times 10^3$
^{120}Sn	4.93	0.5	0.20	29	−997	30	−64
	8.49	43.1	3.40	−98	55	−165	−980
	10.27	7.0	0.31	−660	7	749	−60
	10.68	40.1	1.59	744	52	641	−179
^{122}Sn	5.11	0.4	0.14	24	−997	40	−60
	8.51	38.1	2.98	63	−48	235	969
	10.04	38.6	1.84	−283	43	936	−206
	11.01	20.7	0.75	−957	−41	−260	123
^{124}Sn	5.22	0.3	0.10	21	−998	37	−54
	8.53	29.7	2.31	43	−38	329	943
	9.75	61.7	3.21	−140	50	936	−319
	11.28	11.1	0.37	−989	−30	−118	85

TABLE X

Structure and $\Gamma^{M1}_{0^+\to 1^+}$ widths of excited states $J^\pi = 1^+$ in ^{138}Ba, ^{140}Ce, and ^{142}Nd obtained in TDA

Nucleus	Energy (MeV)	$\Gamma^{M1}_{0^+\to 1^+}$ (eV)	$\Gamma^{M1}_{0^+\to 1^+}$ (W. u.)	pp $1g_{9/2}-1g_{7/2}$	pp $2d_{5/2}-2d_{3/2}$	nn $1h_{11/2}-1h_{9/2}$
				$X\times 10^3$	$X\times 10^3$	$X\times 10^3$
^{138}Ba	4.90	0.6	0.24	−102	994	36
	7.88	4.1	0.41	−911	−79	−404
	9.05	85.6	5.58	−399	−74	914
^{140}Ce	4.84	0.8	0.32	91	−995	−44
	7.86	1.4	0.14	907	64	416
	8.88	75.0	5.17	−411	−78	908
^{142}Nd	4.68	0.9	0.44	73	−996	−51
	7.93	0.01	0.01	862	37	505
	8.71	65.1	4.75	−501	−81	862

TABLE XI

Structure and $\Gamma^{M1}_{0^+\to 1^+}$ widths of excited states $J^\pi = 1^+$ in ^{124}Sn obtained in RPA. Calculation was made using ^{120}Sn radial integrals

Energy (MeV)	$\Gamma^{M1}_{0^+\to 1^+}$ (eV)	$\Gamma^{M1}_{0^+\to 1^+}$ (W. u.)	nn $1g_{9/2}-1g_{7/2}$		nn $2d_{5/2}-2d_{3/2}$		nn $1h_{11/2}-1h_{9/2}$		pp $1g_{9/2}-1g_{7/2}$	
			$X\times 10^3$	$Y\times 10^3$	$X\times 10^3$	$Y\times 10^3$	$X\times 10^3$	$Y\times 10^3$	$X\times 10^3$	$Y\times 10^3$
5.22	0.3	0.13	20	−5	−997	−12	41	−8	−66	−22
8.35	23.1	1.89	40	6	−46	18	332	35	947	97
9.79	57.7	2.96	179	10	−55	−2	−931	−27	316	8
11.31	14.1	0.50	983	0	−32	4	155	−4	−94	5

5. *Results and discussion*

The calculations were performed in RPA and TDA. A few excited $J^\pi = 1^+$ states in the energy region 2.3–12.4 MeV were obtained for each nucleus in question. A characteristic quantity for such a state is the reduced probability B(M1) for transition to the ground state or the width $\Gamma^{M1}_{0^+\to 1^+}$. Energies E, wave functions X, Y and widths $\Gamma^{M1}_{0^+\to 1^+}$ are presented in Tables IV–XI. The excited states $J^\pi = 1^+$ in Sn isotopes and in Ba, Ce and Nd can be divided into two groups:

1. 2.3–7.0 MeV region

The states from this energy region are almost pure two-quasi-particle configurations. Their energies slightly differ from those of unperturbated two-quasi-particle states (Fig. 4). Their widths $\Gamma^{M1}_{0^+\to 1^+}$ are small. Comparatively large values of $\Gamma^{M1}_{0^+\to 1^+}$ (0.10–0.42 W.u.) are a feature of the states originating from levels which differ by the spin direction only ($2d_{5/2}$–$2d_{3/2}$). The other states of this group are two-quasi-particle excitations, $3s_{1/2}$–$2d_{3/2}$ and $2d_{5/2}$–$1g_{7/2}$, and their widths are of the order of 10^{-4}–10^{-5} W.u.

2. 7.0–12.4 MeV region

There are three such states in Sn isotopes and two in Ba, Ce and Nd. First, let us consider the states at energies between 8.5 and 9.0 MeV. Their energies are considerably shifted as compared with those of unperturbated two-quasi-particle states. Electromagnetic transition widths of these states range from 20 eV to 36 eV for Sn isotopes and have values 78, 67, 57 eV for Ba, Ce and Nd, respectively; they are several times greater than the corresponding single-particle widths. The value of the ratio $\Gamma^{M1}_{0^+\to 1^+}/\Gamma^{M1}_{sp,g}$ [1] is 5.05 for ^{120}Sn and 13.2 for ^{140}Ce.

[1] $\Gamma^{M1}_{sp,g}$ stands for effective single-particle electromagnetic transition width calculated for each excited state $J^\pi = 1^+$ according to the formula

$$\Gamma^{M1}_{sp,g} = \frac{\sum_i X^2(i)\Gamma^{M1}_{sp}(i)}{\sum_i X^2(i)}.$$

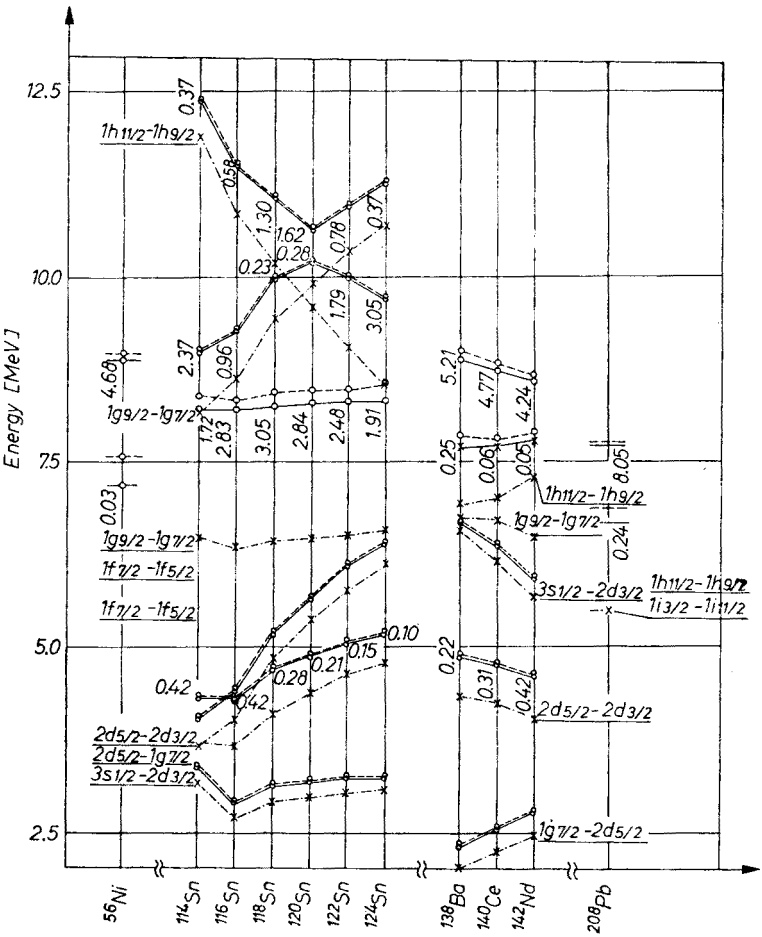

Fig. 4. Excited states $J^\pi = 1^+$. Dot-and-dash line shows the energy of unperturbated two-quasi-particle levels. Solid and dashed lines indicate the energy of states $J^\pi = 1^+$ in RPA and TDA, respectively. The transition widths $\Gamma^{M1}_{0^+\to 1^+}$ are marked if $\Gamma^{M1}_{0^+\to 1^+} \geqslant 0.01$ W. u.

Some of the states in the second group can be considered as collective states. Their widths $\Gamma^{M1}_{0^+\to 1^+}$ are relatively large and range from 0.96 to 3.05 W.u. They are the 9.02, 9.27, 10.97, 10.66, 10,03, 9.74 MeV states in Sn isotopes for $A = 114$, 116, 118, 120, 122, 124, respectively. Let us point out that the states of the second group consist of configurations generated by spin-orbit interaction.

In ^{208}Pb and ^{56}Ni there are two excited states $J^\pi = 1^+$. As a rule the higher states are collective states. They consist of configurations due to spin-orbit splitting. Particularly strong is the 7.82 MeV state in ^{208}Pb, with $\Gamma^{M1}_{0^+\to 1^+} = 80$ eV (8.05 W.u.) and $B(M1)/B_{sp,g}(M1) = 7.5$[2]. Following our results we can see that states of width larger than a tenth of one W.u. are either pure two-quasi-particle configurations generated by

[2] $B^{M1}_{sp,g}$ is calculated in the same way as $\Gamma^{M1}_{sp,g}$.

spin-orbit interaction or a combination of such configurations. The main part (84%–99%) of the electromagnetic M1 transition strength is concentrated on the states of energy within 7.75 to 11.1 MeV. These states should manifest themselves in (N, γ), (γ, N), (N, N'), (e, e') and other reactions.

In tin isotopes and in barium, cerium and neodymium there is a region (4.25–5.25 MeV) which concentrates 2%–9% of the electromagnetic M1 transition strength. It is interesting to point out that such two energy regions are shwn by Gabrakov [7] for deformed nuclei.

Investigation of such states gives us precious information concerning residual spin-spin interaction in atomic nuclei. This knowledge is particularly relevant to the study of many effects generated by this residual interaction.

Comparing the results obtained by RPA and TDA one can see that differences between the two methods are small. This is a general feature of realistic forces [9].

REFERENCES

[1] Z. Bochnacki, S. Ogaza, *Nuclear Phys.*, **69**, 186 (1965).
[2] A. Bohr, B. R. Mottelson, *Nuclear Structure*, Benj. Inc. 1969, v. I, p. 336.
[3] J. Fujita, K. Ikeda, *Nuclear Phys.*, **67**, 145 (1963); J. A. Halbleib, R. A. Sorensen, *Nuclear Phys.*, **A98**, 542 (1967); S. I. Gabrakov, A. A. Kulev, *preprint JINR*, P4-5003, Dubna 1970.
[4] C. S. Shapiro, G. T. Emery, *Phys. Rev. Letters*, **23**, 244 (1969).
[5] S. I. Gabrakov, A. A. Kulev, N. J. Pyatov, *preprint JINR*, E4-4774, Dubna 1969.
[6] S. I. Gabrakov, A. A. Kulev, N. J. Pyatov, *preprint JINR*, E4-4908, Dubna 1970.
[7] S. I. Gabrakov, A. A. Kulev, N. J. Pyatov, D. I. Salamov, G. Schultz, *preprint JINR*, P4-5889, Dubna 1971.
[8] R. A. Broglia, A. Molinari, *Nuclear Phys.*, **A109**, 363 (1963).
[9] M. Jean, *Proc. of Int. Sch. of Phys. "Enrico Fermi"* 1969, p. 171, 239.
[10] E. A. Sanderson, *Phys. Letters*, **19**, 141 (1965).
[11] N. Ullah, D. J. Rowe, *Nuclear Phys.*, **A163**, 257 (1971).
[12] R. D. Woods, D. S. Saxon, *Phys. Rev.*, **95**, 577 (1954).
[13] P. von Brentano, W. K. Dawson, C. F. Moore, P. Richard, W. Whartn, H. Wieman, *Phys. Letters*, **26B**, 666 (1968).
[14] W. Grochulski, private communication.
[15] V. Gillet, A. M. Green, E. A. Sanderson, *Phys. Letters*, **11**, 44 (1964).
[16] A. Bohr, B. R. Mottelson, *Nuclear Structure*, Benj. Inc. 1969, v. I, p. 343.
[17] C. D. Bowman, R. J. Baglan, B. L. Berman, T. W. Phillips, *Phys. Rev. Letters*, **18**, 1302 (1970).
[18] S. T. Belyaev, *Mat. Fys. Medd. Dan. Vid. Selsk.*, **31**, 11 (1959).
[19] S. Ćwiok, M. Wygonowska, *Rapp. UW* IFD/1/72.